Archive of Applied Mechanics 64 (1994) 136–146

Archive of
Applied Mechanics

On the behaviour of rubberlike materials in compression and shear

P. A. J. van den Bogert, Rijswijk and **R. de Borst**, Delft

Summary: The mechanical behaviour of rubberlike materials is modelled in a phenomenological approach using a strain-energy formulation. Nonhomogeneous shear experiments on solid rubber specimens have been carried out as well as simple elongation tests on the same rubber compound. The elongation tests have been used to determine the model constants. By a comparison between experiment and numerical simulation of the nonhomogeneous shear test the predictive capabilities of the Mooney-Rivlin, the Ogden and the Besseling model have been assessed for compression-shear deformation paths. An analytical study explains the numerically observed behaviour.

Über das Verhalten von Gummimaterialien unter Druck und Schubverformungen

Übersicht: Das mechanische Verhalten von Gummimaterialien wird phänomenologisch modelliert unter Anwendung einer Formänderungsenergiefunktion. Es sind nicht-homogene Schubversuche auf dreidimensionale Versuchsproben aus Gummi so wie auch einfache Verlängerungsversuche auf Gummiproben der gleichen Zusammenstellung durchgeführt worden. Die Verlängerungsversuche sind durchgeführt worden um die Stoffkennwerte feststellen zu können. In einer Vergleichung zwischen dem Experiment und der numerischen Simulation von nicht-homogenen Schubversuchen ist die Genauigkeit des Mooney-Rivlinschen Modells, des Ogdenschen Modells und des Besselingschen Modells für kombinierte Druck-Schubverformungen festgestellt worden. In einem analytischen Studium wird das numerisch betrachtete Verhalten auseinandergesetzt.

1 Introduction

Rubber parts are important and often critical components in many engineering structures. Examples are rubber-steel bearings in bridges, shock absorbers, seals between tunnel segments, et cetera [1, 2]. Typically, these rubber parts are loaded in a combination of compression and shear. Considering the classical constitutive theories that have been developed for rubberlike materials this is somewhat unfortunate, since the experimental basis of these models, e.g., those of Mooney [3], Rivlin [4], Blatz and Ko [5] and Besseling [6], are uniaxial [7] and biaxial extension experiments [8]. The question thus arises if, and if yes to which extent, these models are applicable to deformation paths as experienced by such rubber parts mentioned above.

Traditionally, rubber materials have been modelled using hyperelastic concepts, with the strain energy function only dependent upon the deviatoric deformations. This assumption of incompressibility is normally motivated by the observation that rubberlike materials show an extremely high resistance to volumetric deformations compared with that to deviatoric deformations. However, it may be questioned whether this assumption still holds when rubber parts are loaded up to high compressive deformation levels, or whether volume changes should then be included in the strain energy formulation [9, 10]. In sum, we wish to investigate whether the strain energy functions postulated by Mooney [3], Rivlin [4] and others, are sufficiently flexible and general to accurately model compressive and shear loadings in rubbers and which possible modifications or extensions must be made in order to obtain a sufficiently general formulation for rubberlike materials.

In this paper we shall investigate a number of strain-energy functions with respect to their ability to predict a wide range of loading conditions [3, 4, 6, 8]. Uniaxial tests will be utilised to derive the model parameters of the strain energy function, which will subsequently be used to assess the model's performance in non-homogeneous compression-shear experiments [1, 11, 12]. The inhomogeneous

character of the compression-shear experiments requires a numerical method for an accurate prediction. The finite element procedures used in these simulations have been described in [1, 13].

The paper is organised as follows. Firstly, a concise overview is given of the various constitutive formulations available for rubberlike materials. Next, the uniaxial elongation experiments that have been carried out [11, 12] are discussed briefly and the model parameters of the constitutive formulations used are determined. Then, a discussion follows of the numerical simulation of the non-homogeneous compression-shear experiments and the correlation with experimental evidence. The contribution is concluded with an analytical study into some salient characteristics of the Mooney-Rivlin [3, 4], the Besseling [6] and the Ogden [8] models under homogeneous shear loadings in order to explain the numerically observed phenomena.

2 Constitutive models for rubberlike materials

For an isotropic elastic material the strain-energy function W can be described by a set of basic parameters χ. These parameters can either be invariants of a deformation tensor (here the invariants I_1, I_2 and I_3 of the right Cauchy-Green stretch tensor $\mathbf{C}$), or its principal stretches λ_1, λ_2 and λ_3. In a compact manner the strain-energy function is written as

$$W = W(\chi). \tag{1}$$

When introducing a strictly separated strain-energy function the total deformation must be split into a volumetric contribution and a deviatoric part, which can be accomplished by introducing a modified set of basic parameters $\tilde{\chi}$. In case of a representation in terms of invariants we have

$$J_1 = I_1 I_3^{-1/3} \tag{2}$$

and

$$J_2 = I_2 I_3^{-2/3}, \tag{3}$$

while with a representation in principal stretches we can define the modified principal stretches as,

$$\tilde{\lambda}_i = \lambda_i I_3^{-1/6}, \quad i = 1, 2, 3. \tag{4}$$

Either representation can be utilised to define the purely deviatoric part of the strain energy function $W_d(\tilde{\chi})$. The relative volume change,

$$J = \sqrt{\det(\mathbf{C})}, \tag{5}$$

is used to describe the hydrostatic part of the strain-energy formulation $W_h(J)$. Assuming that the strain-energy function can be decomposed into a part that is entirely dependent upon deviatoric deformations and a contribution that stems from the relative volume change J, we have

$$W = W_d(\tilde{\chi}) + W_h(J). \tag{6}$$

Typically, W_d is $O(\mu)$ and W_h is $O(\varkappa)$, $\mu \ll \varkappa$ for rubberlike materials, μ and $\varkappa$ being the groundstate shear modulus and the bulk modulus of the rubber, respectively. If a strict decomposition of the strain energy function into a deviatoric part and into a volumetric component cannot be carried through, a coupling function $W_c(\chi)$ should be added to the right-hand side of eq. (6). However, numerical studies [1] suggest that even for cases where we have intense levels of compression and shear, the effect of such a refinement remains negligible in practical engineering cases.

The second Piola-Kirchhoff stress $\boldsymbol{\sigma}$ can be calculated by differentiation of W with respect to the Right Cauchy-Green stretch tensor

$$\boldsymbol{\sigma} = \boldsymbol{\sigma}_d + \boldsymbol{\sigma}_h, \tag{7}$$

with

$$\boldsymbol{\sigma}_d = 2 \frac{\partial W_d}{\partial \mathbf{C}} \tag{8}$$

and

$$\boldsymbol{\sigma}_h = 2p \frac{\partial J}{\partial \mathbf{C}}. \tag{9}$$

In (9) p is the hydrostatic pressure. For the present purpose the formulation of the hydrostatic part is not important as long as $\varkappa \gg \mu$, and a simple, linear relationship has been adopted [2]. On the other hand, the precise formulation of the deviatoric component of the strain-energy function is important. Two types of formulations have been considered. The first are the invariant-based models of Mooney-Rivlin [3, 4] and Besseling [6]:

$$W_d = K_1(J_1 - 3)^m + K_2(J_2 - 3), \tag{10}$$

with m, K_1 and K_2 material parameters. For the Mooney-Rivlin formulation, $m = 1$ and $2(K_1 + K_2) = \mu$. The other approach is the one by Ogden [8], which employs principal stretches to describe the strain-energy function:

$$W_d = \sum_r^{n_r} \frac{\mu_r}{\alpha_r} (\tilde{\lambda}_1^{\alpha_r} + \tilde{\lambda}_2^{\alpha_r} + \tilde{\lambda}_3^{\alpha_r} - 3), \tag{11}$$

with μ_r and α_r model parameters. The Ogden formulation is very flexible and data from uniaxial tests are fitted accurately and in a natural fashion. Its generality also becomes apparent since many other formulations can be retrieved as special cases of the Ogden model. For instance, when setting $n_r = 1$ and $\alpha_1 = 2$ the neo-Hookean formulation is obtained, while $n_r = 2$ with $\alpha_1 = 2$ and $\alpha_2 = -2$ results in the Mooney-Rivlin formulation of (10). The disadvantage of the Ogden formulation, and in fact of any hyperelastic model expressed in principal stretches, are the difficulties involved in properly implementing the model in a general three-dimensional context. Difficulties arise when two or more principal stretches become equal, since then the denominator of the derivative of the principal stretch with respect to the invariants, which expression is needed in the solution process, becomes zero.

3 Uniaxial elongation

For many materials the simple tensile test is used to extract a limited number of model parameters. When used in an appropriate constitutive model, the material response should be captured for a large number of strain paths. In this section model parameters for a number of deviatoric models are determined from uniaxial tension tests. In a subsequent section the validity of this approach for rubberlike materials is discussed.

On the basis of the experiments carried out at the TNO Centre for Polymeric Materials [11, 12] a least squares fit of model constants has been carried out for different ranges of λ and for various deviatoric models. The experimental programme consisted of uniaxial elongation tests on a number of identical rubber specimens which have been vulcanised during 30, 45 and 60 minutes respectively at 140 °C. Secondly, shear tests and compression-shear tests have been carried out on samples of the same rubber compound which has been vulcanised during 45 minutes at 140 °C. For the uniaxial elongation tests the force-deformation relation has been measured in the first and fifth loading cycle, executed at a speed of 5 mm/min. Unless specified otherwise the measurements in the fifth cycle were used in the parameter identification in order to account for the Mullins effect [14].

The Mooney-Rivlin approximation is accurate only for a small deformation range. This is caused by the inability of the model to describe the inflexion point in the force-stretch relation. Therefore, the upper limit of the validity range is set to $\lambda = 1.5$. When the upper boundary is moved to $\lambda = 2.0$ a negative value for K_2 results and a physically irrelevant force prediction in the compressive regime is observed [1]. By shifting the lower boundary from $\lambda = 1.0$ to $\lambda = 1.15$ the constants K_1 and K_2 change significantly, while only a small influence is observed on the force prediction. Since the experimental error is relatively large in the neighbourhood of $\lambda = 1$ it is reasonable to use the range $1.15 \leqq \lambda \leqq 1.5$. The parameters obtained by a least squares fit for measurements in this deformation range are listed in Table 1 [1]. The a-fit corresponds to measurements in the fifth loading cycle and the b-fit derives from experimental data obtained in the first loading cycle. In Table 1, the last column gives the ground-state shear modulus μ.

Table 1. Model constants of the different rubber models determined for a compound that has been vulcanised for 45 minutes

	Mooney	K_1	K_2			μ
a-fit	5th cycle	0.1486	0.4849			1.267
b-fit	1st cycle	0.3198	0.3370			1.314
	Besseling	K_1	K_2	m		μ
	$1.15 \leqq \lambda \leqq 2.0$	0.02493	0.6714	2.946		1.343
	Ogden	μ_1	α_1	μ_2	α_2	μ
a-fit	$1.15 \leqq \lambda \leqq 2.0$	−1.443	−1.787	$2.741 \cdot 10^{-3}$	9.581	1.303
b-fit	$1.00 \leqq \lambda \leqq 2.0$	−0.9952	−2.713	$2.053 \cdot 10^{-3}$	9.905	1.360
c-fit	pos. powers	3.164	0.5	0.0486	5.5	0.925

For the Besseling and the Ogden models the upper boundary need not be restricted to $\lambda = 1.5$ since they are capable of modelling the increasing stiffness for higher stretches. For the Ogden model a two-term expansion is sufficient to obtain a close resemblance with the experiment. Additional terms cannot be motivated when only simple elongation tests are considered. The results for a fit on $1.15 \leqq \lambda \leqq 2.0$ is given in Table 1 for both models, while an additional parameter set is listed for the Ogden model based on a fit in the 'window' $1.0 \leqq \lambda \leqq 2.0$ (b-fit).

In Figure 1 the experimental force-stretch relation is given (solid line) for the specimen after 45 minutes vulcanisation. Also, the force evolution has been plotted according to the Mooney-Rivlin, the Ogden and the Besseling models. The corresponding model constants are listed in Table 1.

For all the models for the deviatoric strain energy that have been considered different sets of constants can match the uniaxial stress development reasonably well, *cf.* the Ogden model in Table 1. In a different strain situation, however, different parameter sets may lead to significant deviations of the stress prediction. Since the major goal is to obtain a constitutive model that is reliable for any strain situation the validity domain should be ascertained beyond the class of uniaxial experiments. That is, the predictive power of the model, the constants and the way to calculate them, must be validated by experimental evidence for a wide range of loading conditions. Only then, the reliability of structural analyses with a three-dimensional strain situation in tension *and compression* can be increased.

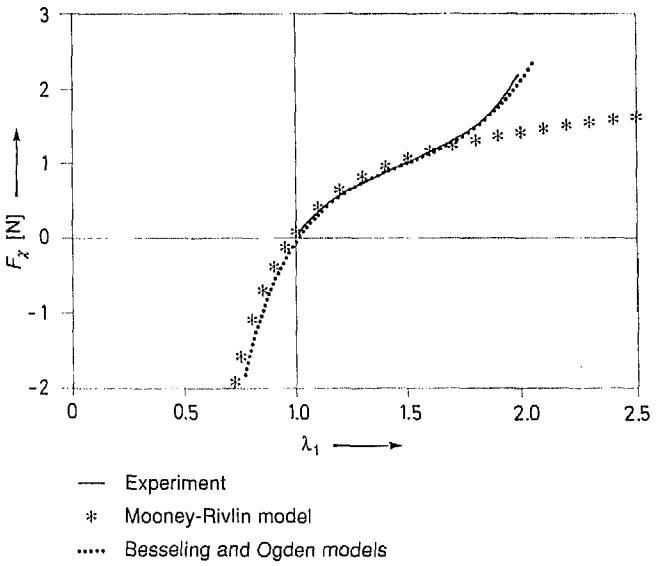

Fig. 1. Least squares fit of the Mooney-Rivlin model fitted in the range $1.15 \leqq \lambda \leqq 1.5$, and the Ogden and Besseling models fitted in the range $1.15 \leqq \lambda \leqq 2.0$

4 Non-homogeneous shear deformation

4.1 Description of the shear experiment

For the shear and compression-shear experiments a composition of four specimens of $10 \times 20 \times 20\ mm^3$ has been used, Figure 2. A rigid connection with the steel members is established at the upper and lower face of the rubber samples during the vulcanisation period. The compound for the rubber samples is identical to that of the samples of the uniaxial elongation experiments and has been vulcanised during 45 minutes at 140°C [12].

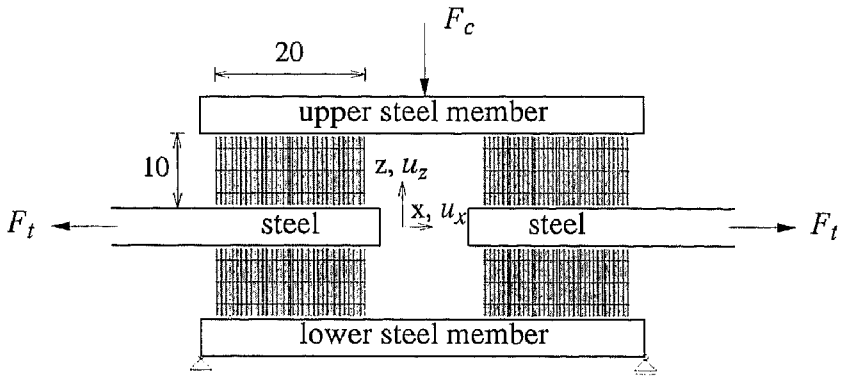

Fig. 2. Composition of the test specimen (dimensions in [mm])

In the middle of the steel members a horizontal displacement has been imposed with a speed of 10 mm/mm until $u_x = 30$ mm. So, each specimen undergoes a shear displacement of 15 mm, which implies a shear angle larger than 45° in the final state. In the experiments that will be discussed here the deformation in the vertical direction (z-direction) is free. Other boundary conditions in the vertical direction with a prescribed vertical compressive displacement of 0, 9.6 and 15.5 mm are considered in [1]. The outcome of these experiments is qualitatively fully in line with the observations and simulations of the free contraction experiment described here and is therefore not treated further.

4.2 Numerical aspects of the simulation

For the numerical simulation of the shear experiment one half of a rubber specimen is modelled with 192 solid elements, Figure 3. Use is made of the 20/4 hexahedron elements with a quadratic displacement field (20 nodes, 60 displacement degrees-of-freedom) and 4 pressure degrees-of-freedom [1, 13]. A $3 \times 3 \times 3$ Gauss scheme is used for the integration of the elements. In the plane of symmetry

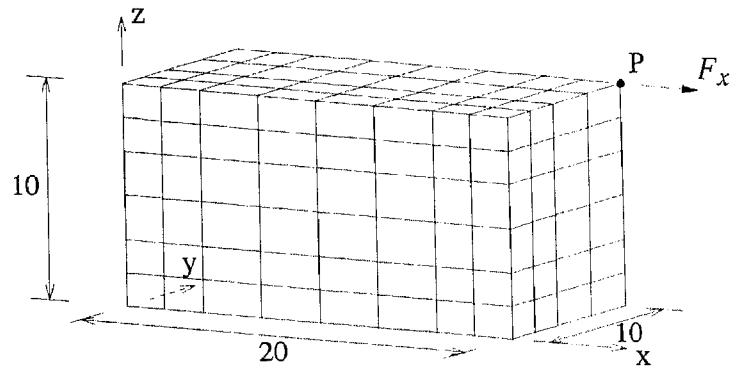

Fig. 3. Finite element mesh with 192 quadratic 20/4 elements

$y = 10$ mm the displacement $u_y = 0$ is prescribed. In the bottom plane, at $z = 0$, all displacements and in the top plane, at $z = 10$ mm, the displacements u_y are prevented. The top plane is allowed to displace rigidly in the x and z-directions. In point P a shear force in the x-direction is applied.

4.3 *Correlation between experiment and simulation*

For the free contraction experiment the tensile force F_t, the extension deformation u_x and the lateral deformation u_z of the composition of rubber samples have been measured in the first and fifth loading cycle. In Figure 4 a F_t and u_x have been scaled and compared with F_x and u_x from a simulation of the shear experiment with a Mooney-Rivlin model [3, 4]. In the experimental results a softer response and a diminished hysteresis is observed for a higher number of loading cycles. The initial stiffness predicted by the Mooney-Rivlin model is a little higher than in the experimental results. The ultimate experimental deformation in the first cycle is close to the curve of the numerical simulation of the first cycle, but the agreement in the fifth cycle is less good. Except for the initial stiffness the resemblance between the corresponding experimental and numerical curves is rather poor. From the experimental curve it is observed that the stiffness will increase at larger shear deformations, while the Mooney-Rivlin is only able to predict a monotonically decreasing stiffness. At this point the same restrictions are encountered for the Mooney-Rivlin model as in the uniaxial deformation experiment. In fact, the good correspondence in the ultimate deformation state can be qualified as coincidental. With the Mooney-Rivlin model it is not possible to predict the shape of the load-deformation curve accurately.

In Figure 4 b the evolution of the lateral deformation has been plotted. In this diagram a positive value for u_z is a displacement in the direction of the positive z-axis, that is an uplift of the top plane. It is found that the prediction of the vertical displacement u_z of the upper steel member is much different when the first or the fifth loading cycle is simulated. This significant change is caused by a major shift in the relative contributions of the constants K_1 and K_2 to the groundstate shear modulus (Table 1). In fact, the difference in the relation F_x-u_z between the first and the fifth loading cycle is of the same order as for the relation between F_x and u_x. For the Mooney-Rivlin model any agreement with the experimental results is lost, owing to the model property which prevents the prediction of height reduction in shear.

Next, the Besseling model [6] is considered. In Figure 5 the horizontal and vertical displacements have been plotted versus the applied shear force. The improvement over the Mooney-Rivlin formulation is clear: the F_x-u_x-curve is now simulated correctly, i.e. an increasing stiffness is calculated

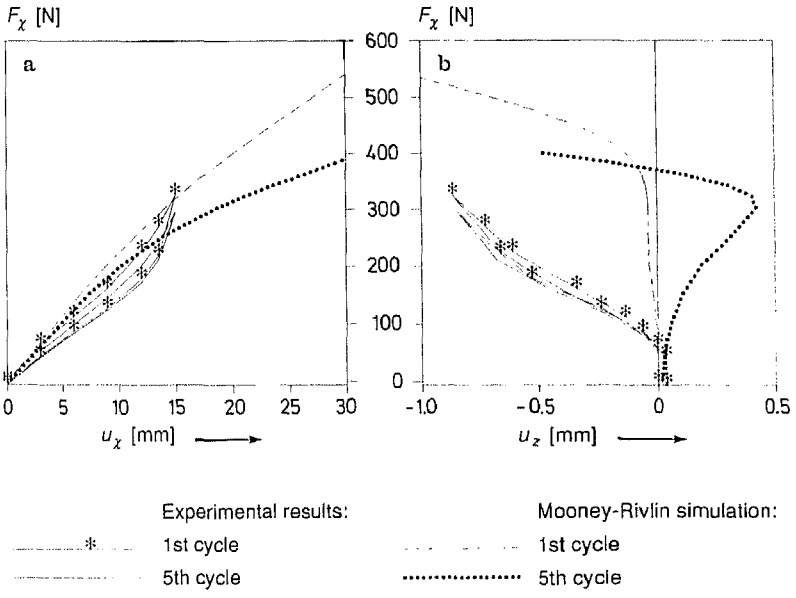

Fig. 4. The applied shear force F_x related to a) the horizontal displacement u_x and b) the vertical displacement u_z of point P for the Mooney-Rivlin model [3, 4]

at higher load levels. However, the computed F_x-u_z-relation shows that this model is not capable of simulating a height reduction of the specimen either.

Finally, similar analyses have been carried out for the Ogden model [8] using the model constants of Table 1. It is recalled that the constants have been determined from the same uniaxial elongation experiment as for the Mooney-Rivlin and Besseling models. The computed relations for $F_x - u_x$ and $F_x - u_z$ are given in Figures 6a und 6b respectively. Over the whole deformation range a somewhat stiff response is predicted when the constants are substituted according to the a-fit and b-fits of the uniaxial elongation data (Table 1). The small discrepancy between the numerical and experimental stiffness in the undeformed state is of the same order as for the Mooney-Rivlin and Besseling models. The improvement of the Ogden model concerns the shape of the computed F_x-u_x-curve, which can be made in keeping with the experimental findings.

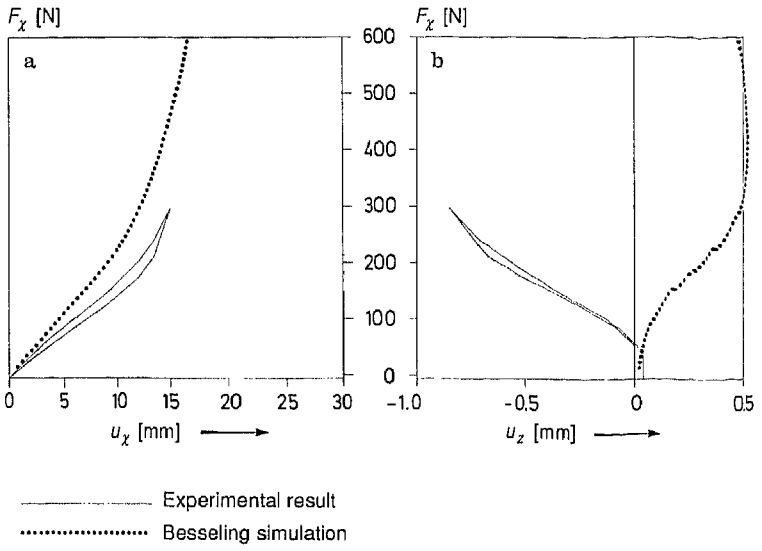

Fig. 5. The applied shear force F_x related to a) the horizontal displacement u_x and b) the vertical displacement u_z of point P for the Besseling model [6]

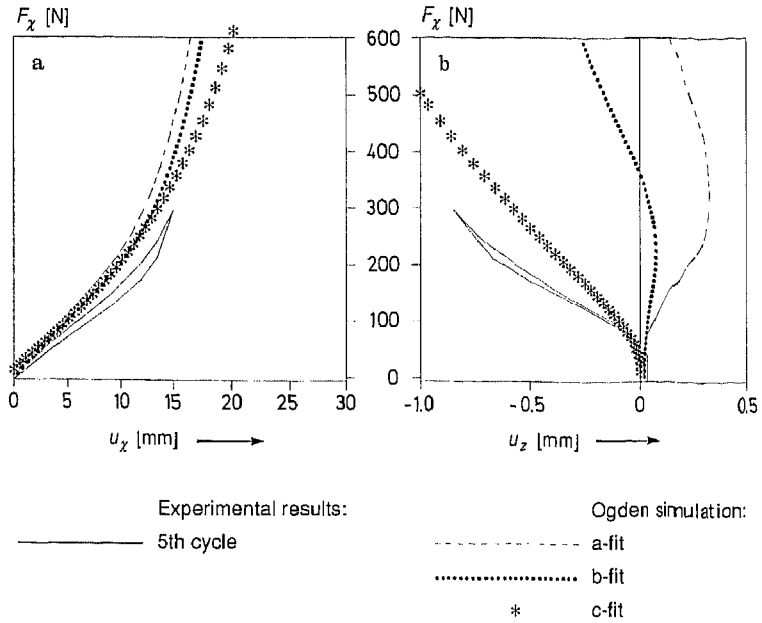

Fig. 6. The applied shear force F_x related to a) the horizontal displacement u_x and b) the vertical displacement u_z of point P for the Ogden model [8]

In Figure 6 b the vertical displacement is plotted against the applied shear force. It is seen that the predicted vertical displacement of the specimen is not in correspondence with the experimental results when the a-fit and b-fit constants are used. To demonstrate the capability of the Ogden model to simulate a vertical contraction of the rubber specimens the constants μ_1 and μ_2 of the Ogden model are calculated by a least squares fit to the uniaxial elongation data with fixed values for the powers, namely $\alpha_1 = 0.5$ and $\alpha_2 = 5.5$ (c-fit in Table 1). The resemblance with the experimental uniaxial elongation curve is now slightly less than for the case when all model parameters are fitted. However, for the shear experiment the computed relations for the shear force versus the horizontal and versus the vertical displacement are in much better agreement with the experimental results. This shows that model constants derived from an optimal fit of uniaxial elongation experiments do not necessarily predict the shear deformation correctly. A uniaxial elongation experiment simply does not provide enough information to obtain an accurate simulation of the shear test. This is confirmed by the observation that more than one set of model parameters give reasonable fits in uniaxial elongation for the Mooney-Rivlin and the Ogden models.

5 Homogeneous shear deformation

To explain the numerical results of the nonhomogeneous shear experiments that have been presented in the previous section we shall study the characteristics of the various formulations for the deviatoric part in a simulation of a shear test under the assumption of homogeneous deformations, Figure 7. Because of the boundary conditions $\sigma_{22} = \sigma_{33} = 0$ the vertical and transverse stretch components λ_2 and λ_3 are unknown.

The shear deformation can be represented by the deformation gradient $\mathbf{F}$

$$\mathbf{F} = \begin{bmatrix} 1 & \Delta u & 0 \\ 0 & \lambda_2 & 0 \\ 0 & 0 & \lambda_3 \end{bmatrix}. \tag{12}$$

For the stretch tensor $\mathbf{C}$ the invariants then read

$$I_1 = \lambda_2^2 + \lambda_3^2 + \Delta u^2 + 1, \tag{13}$$

$$I_2 = \lambda_2^2 + \lambda_3^2 + (\lambda_3 \Delta u)^2 + (\lambda_2 \lambda_3)^2, \tag{14}$$

$$I_3 = (\lambda_2 \lambda_3)^2, \tag{15}$$

so that we obtain for the derivatives with respect to $\mathbf{C}$:

$$\partial I_1 / \partial \mathbf{C} = 0, \tag{16}$$

$$\frac{\partial I_2}{\partial \mathbf{C}} = [\lambda_2^2 + \lambda_3^2 + \Delta u^2,\ 1 + \lambda_3^2 + 1,\ 1 + \lambda_2^2 + \Delta u^2,\ -\Delta u,\ 0,\ 0]^T, \tag{17}$$

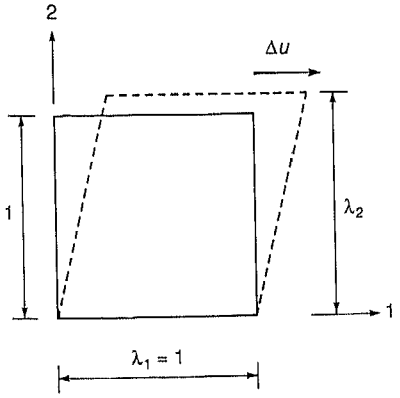

Fig. 7. Homogeneous shear deformation experiment

and

$$\frac{\partial I_3}{\partial \mathbf{C}} = [\lambda_2{}^2\lambda_3{}^2 + \lambda_3{}^2\Delta u^2,\ \lambda_3{}^2,\ \lambda_2{}^2,\ -\lambda_3{}^2\Delta u,\ 0,\ 0]^T. \tag{18}$$

The stress components are calculated by substituting (13)–(18) into eqs. (7)–(9). The stretches λ_2 and λ_3 are subsequently solved from the boundary conditions $\sigma_{22} = 0$ and $\sigma_{33} = 0$. To eliminate the stress contribution that stems from the volumetric part of the strain energy function (W_h, (9)), we subtract $\beta^2\sigma_{33}$ from σ_{22}, with $\beta = \lambda_3/\lambda_2$. Thus, we have

$$\sigma_{22} - \beta^2\sigma_{33} = 0. \tag{19}$$

For the invariant-based models proposed by Mooney and Rivlin [3, 4] and by Besseling [6], which are characterised by the strain-energy function (10), it can be derived that

$$\sigma_{22} - \beta^2\sigma_{33} = 2(1 - \beta^2)\,\alpha^{-1}[m(J_1 - 3)^{m-1}\,K_1\alpha^{1/3} + K_2\alpha^{-1/3}] - 2K_2\alpha^{-4/3}\beta^2\Delta u^2 \tag{20}$$

with $\alpha = \lambda_2\lambda_3$. With condition (19) we obtain

$$\beta^{-2} = 1 + \frac{K_2\alpha^{-1/3}}{m(J_1 - 3)^{m-1}\,K_1\alpha^{1/3} + K_2\alpha^{-1/3}}\,\Delta u^2, \tag{21}$$

with $m = 1$ for the Mooney-Rivlin model [3, 4]. Invoking the condition $\sigma_{33} = 0$ we obtain, using a linear hydrostatic model, a second relation between λ_2 and λ_3

$$\lambda_3 = \lambda_2{}^{-1} - \frac{\sigma_{33-d}}{\varkappa\lambda_2}, \tag{22}$$

with σ_{33-d} the part of σ_{33} that stems from the deviatoric part of the strain-energy function W_d. Since $\varkappa \gg \mu$ we can neglect the second part on the right hand side of (22), and relation (21) can be simplified to

$$\lambda_2{}^4 = 1 + \frac{K_2}{m(J_1 - 3)^{m-1}\,K_1 + K_2}\,\Delta u^2. \tag{23}$$

This relation shows an important property of the Mooney-Rivlin [3, 4] and Besseling [6] models. Since Δu^2 is positive and $K_1 + K_2 = \frac{1}{2}\mu$ for the Mooney-Rivlin model, and $K_2 = \frac{1}{2}\mu$ for the Besseling model, the second term of the right-hand side of (23) will always be positive. Therefore, whether λ_2 will be less or greater than 1 depends on the sign of K_2. In [1] it has been demonstrated that a negative value for K_2 in the Mooney-Rivlin model yields physically unrealistic answers in uniaxial deformation experiments when $\lambda < 1$. For the Besseling model K_2 will never be negative. As a consequence, the Mooney-Rivlin [3, 4] and the Besseling [6] models predict a shear deformation which is necessarily accompanied by an upward movement of the top surface. This is at odds with the experimental results of the previous section, where a reduction of the height is observed, but fully explains the results of the numerical simulations with these models.

In the same manner an analytical solution can be derived for the Ogden [8] model. The results are presented in Figure 8, where the vertical displacement of the top plane is plotted as a function of the relative shear displacement $\Delta u/h$, with h the height of the specimen. The Ogden expansion is restricted to a single term with $2\mu = \mu_1\alpha_1 = 1$. It is seen that a simple shear deformation with a strictly horizontal displacement of the top plane is obtained for $\alpha_1 = 2$. This Ogden expansion is equivalent with the term $J_1 - 3$ in the Mooney-Rivlin model, that is when only $K_1 \neq 0$, the neo-Hookean form. When only $K_2 \neq 0$ an upward movement is found as given by the curve $\alpha_1 = -2$ in Figure 8. In the Mooney-Rivlin formulation the K_2-part is thus responsible for the uplift of the top plane, while the K_1-term does not have any influence on the vertical displacement. However, when $\alpha_1 > 2$ a downward displacement is simulated, so that the Ogden model is more flexible in describing shear deformations than the Mooney-Rivlin and the Besseling models.

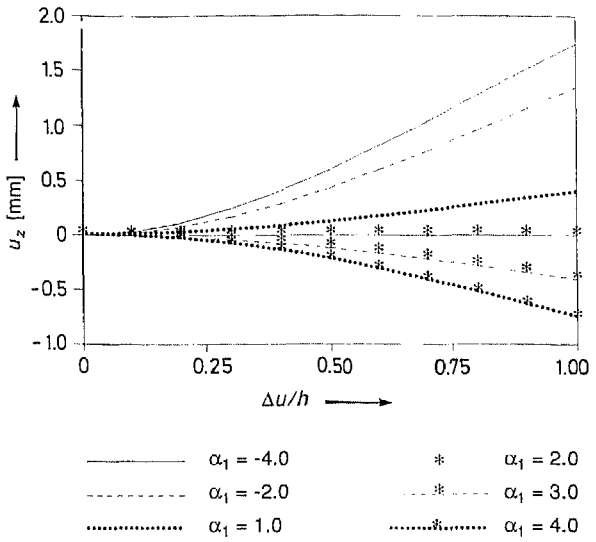

Fig. 8. The vertical displacement as a function of the relative shear deformation for various values of α_1 in the Ogden model [8]

6 Concluding remarks

Recent studies have shown that the hydrostatic part W_h and the coupling function W_c in the strain-energy function have a negligible influence on the predicted load-displacement curves of solid rubber specimens loaded in a combination of shear and compression [1]. Consequently, the behaviour of rubber specimens for such loading paths is almost completely described by the deviatoric part of the strain-energy function. In view of their inability to correctly predict the vertical displacement u_z in shear-compression experiments it seems that the Mooney-Rivlin [3, 4] and Besseling models [6] for the deviatoric part of the strain energy function W_d are less appropriate for the analysis of rubber components loaded in shear and in combined compression-shear loadings. On the other hand, the Ogden model [8] is capable of predicting the height reduction that accompanies a shear deformation for nearly incompressible rubberlike materials.

References

1. Bogert, P. A. J. van den: Computational modelling of rubberlike material behaviour. Dissertation, Delft University of Technology, 1991
2. Borst, R. de; Bogert, P. A. J. van den; Zeilmaker, J.: Modelling and analysis of rubberlike materials. Heron 33 (1988)
3. Mooney, M.: A theory of elastic deformations. J. Appl. Physics 11 (1940) 582
4. Rivlin, R. S.: Large elastic deformations of isotropic materials, fundamental concepts. Phil. Trans. Roy. Soc. Soc./A 240 (1948) 459–490
5. Blatz, P. J.; Ko, W. L.: Application of finite elasticity theory to the deformation of rubber materials. Trans. Soc. Rheology 6 (1962) 223–251
6. Besseling, J. F.: Finite element properties based upon elastic potential interpolation. In: Atluri, S. N.; Gallagher, R. H.; Zienkiewicz, O. C. (eds.) Hybrid and Mixed Finite Element Methods, pp. 253–266. New York: Wiley and Sons 1983
7. Peng, S. T. J.; Landel, R. F.: Stored energy function of rubberlike materials derived from simple tensile data. J. Appl. Physics 43 (1972) 3063–3067
8. Ogden, R. W.: Large deformation isotropic elasticity: on the correlation of theory and experiment for incompressible rubberlike solids. Proc. Roy. Soc. London/A 326 (1972) 565–584
9. Ogden, R. W.: Volume changes associated with the deformation of rubberlike solids. J. Mech. Phys. Solids 24 (1976) 323–338
10. Peng, S. T. J.; Landel, R. F.: Stored energy function and compressibility of compressible rubberlike materials under large strain. J. Appl. Physics 46 (1975) 2599–2604
11. Steen, J.: Testing rubber composition (in Dutch), Report 820/89, TNO Centre for Polymeric Materials, Delft, 1989
12. Bogert, P. A. J. van den: Rubber specimen loaded in shear and compression; experiment and calculation. Report 25.2.89.22, Delft University of Technology, Delft, 1990

13. Bogert, P. A. J. van den; Borst, R. de; Luiten, G. T.; Zeilmaker, J.: Robust finite elements for 3D-analysis of rubberlike materials. Engng. Comput. 8 (1991) 3–17
14. Mullins, L.: Effect of stretching on the properties of rubber. J. Rubber Research 16 (1947) 275–289

Received Juni, 28, 1993

Dr. P. A. J. van den Bogert
Shell Research B. V.
P. O. Box 60
2280 AB Rijswijk
The Netherlands

Prof. Dr. R. de Borst
Delft University of Technology,
Faculty of Civil Engineering/TNO Building and Construction Research
P. O. Box 5048, 2600 GA Delft
The Netherlands